Geophysical Research Letters

RESEARCH LETTER
10.1029/2022GL101203

The Impact of Winds on AMOC in a Fully-Coupled Climate Model

Lettie A. Roach[1,2], Edward Blanchard-Wrigglesworth[3], Sarah Ragen[4], Wei Cheng[5,6], Kyle C. Armour[3,4], and Cecilia M. Bitz[3]

[1]NASA Goddard Institute for Space Studies, New York, NY, USA, [2]Center for Climate Systems Research, Columbia University, New York, NY, USA, [3]Department of Atmospheric Sciences, University of Washington, Seattle, WA, USA, [4]School of Oceanography, University of Washington, Seattle, WA, USA, [5]Cooperative Institute for Climate, Ocean, and Ecosystem Studies, University of Washington, Seattle, WA, USA, [6]NOAA Pacific Marine Environmental Laboratory, Seattle, WA, USA

Key Points:

- We nudge winds above the boundary layer toward reanalysis in a fully-coupled climate model over various spatial domains
- Constraining winds north of 45°N reduces biases in subpolar gyre surface buoyancy fluxes and Atlantic Meridional Overturning Circulation (AMOC) at 26.5°N
- Wind-nudging experiments capture observed phasing of AMOC interannual variability at 26.5°N, but underestimate variability across timescales

Supporting Information:

Supporting Information may be found in the online version of this article.

Correspondence to:

L. A. Roach,
l.roach@columbia.edu

Citation:

Roach, L. A., Blanchard-Wrigglesworth, E., Ragen, S., Cheng, W., Armour, K. C., & Bitz, C. M. (2022). The impact of winds on AMOC in a fully-coupled climate model. *Geophysical Research Letters*, *49*, e2022GL101203. https://doi.org/10.1029/2022GL101203

Received 7 SEP 2022
Accepted 22 NOV 2022

Abstract Here we investigate the role of the atmospheric circulation in the Atlantic Meridional Overturning Circulation (AMOC) by comparing a fully-coupled large ensemble, a forced-ocean simulation, and new experiments using a fully-coupled global climate model where winds above the boundary layer are nudged toward reanalysis. When winds are nudged north of 45°N, agreement with RAPID array observations of AMOC at 26.5°N improves across several metrics. The phasing of interannual variability is well-captured due to the response of the local Ekman component in both wind-nudging and forced-ocean simulations, however the variance remains underestimated. The mean AMOC strength is substantially reduced relative to the fully-coupled model large ensemble, which is biased high, due to the impact of winds on surface buoyancy fluxes over the subpolar gyre. Nudging winds toward observations also reduces the 1979–2016 trend in AMOC, suggesting that improvement in the representation of the high-latitude atmosphere is important for projecting long-term AMOC changes.

Plain Language Summary The Atlantic Meridional Overturning Circulation (AMOC) is a system of ocean currents that transports warm water northward near the ocean surface and cold water southward at depth, impacting a number of aspects of global climate. We focus on the strength of this circulation at 26.5°N, the location of an observing system. Coupled climate models, including the one we use here (CESM1), have biases in AMOC strength compared to these observations. We find that constraining CESM1 to observed winds in the mid-to-high northern latitudes improves the simulation of AMOC across several metrics. This highlights the importance of winds for various aspects of this oceanic circulation system, including its year-to-year variations, mean strength and multi-year trends.

1. Introduction

The Atlantic Meridional Overturning Circulation (AMOC) is a system of currents that extends from the Southern Ocean to the Nordic Seas, transporting warm water northward near the surface and cold water southward at depth. It is a fundamental component of the global climate system, impacting a host of climate phenomena from Arctic sea ice to the Indian Monsoon (see Zhang et al. (2019) for a review of climate impacts). AMOC is projected to weaken over the 21st century (Cheng et al., 2013; Weijer et al., 2020), but with low confidence in the timing and magnitude of the decline (Fox-Kemper et al., 2021).

Many previous studies highlight the importance of atmospheric circulation for variability in AMOC across timescales (see Buckley and Marshall (2016) for a review). It is understood that interannual AMOC variability is primarily driven by momentum forcing, while decadal and longer timescales are primarily driven by buoyancy forcing (e.g., Larson et al., 2020; Roberts et al., 2013; Yeager and Danabasoglu, 2014). AMOC variability at 26.5°N is dominated by sub-annual to interannual variations in momentum forcing through local winds (Kostov et al., 2021; Larson et al., 2020; Roberts et al., 2013; Yeager & Danabasoglu, 2014). On longer timescales, there is a contribution from non-local buoyancy forcing, largely from subpolar latitudes (Delworth et al., 2016; Kostov et al., 2021; Yeager & Danabasoglu, 2014). Changes in atmospheric circulation drive changes in both buoyancy and momentum forcing, with a dominant role for the North Atlantic Oscillation (NAO) and its associated turbulent heat fluxes (e.g., Oldenburg et al., 2021; Oldenburg et al., 2022).

The most recent generation of coupled climate models simulate a large range of mean AMOC strengths (Fox-Kemper et al., 2021; Weijer et al., 2020) and generally underestimate interannual and decadal variability (Fox-Kemper et al., 2021; Roberts et al., 2014; Wang et al., 2017; Yan et al., 2018). Because of the wide-ranging climate impacts arising from AMOC, understanding why coupled climate models differ from observations is critical for interpreting and improving global climate projections over the 21st century. A "nudging," or "relaxation," approach has been widely used previously to diagnose the origin of errors in atmospheric variables (e.g., Jung et al., 2010; Jung et al., 2014; Liu et al., 2021). For example, Jung et al. (2010) nudge various model fields toward reanalysis over different spatial domains to diagnose the remote impact of error reduction in those regions on winds and geopotential heights. Roach and Blanchard-Wrigglesworth (2022) apply wind-nudging north of 60°N to a fully-coupled climate model to highlight biases in sea ice trends that cannot be ascribed to biases in atmospheric circulation. Nudging the winds in a coupled climate model toward observed winds constrains the circulation but permits the atmosphere to respond thermodynamically to surface conditions. This method maintains the coupled atmosphere-ocean interactions in surface fluxes, which are not represented in forced-ocean models where near-surface atmospheric conditions are prescribed.

Given that winds have been shown to be a leading driver of AMOC, here we apply wind-nudging to investigate the causes of biases in simulating AMOC in the fully-coupled Community Earth System Model version 1 (CESM1). We focus on the AMOC at 26.5°N so that results can be compared with observations from the RAPID array. We present experiments with CESM1 over the recent historical period where model winds are nudged toward values from reanalysis above the boundary layer over various spatial domains polewards of 45°, to assess the role of high-latitude winds in driving subtropical AMOC. Differences between these nudged-wind experiments and the CESM1 Large Ensemble (LENS) mean (Kay et al., 2015) reveal the impact of observed high-latitude atmospheric circulation on AMOC changes relative to the modeled forced response.

2. Methods

We use the National Center for Atmospheric Research (NCAR) Community Earth System Model version 1 with the Community Atmosphere Model version 5 (CESM1-CAM5) (Hurrell et al., 2013) (one of the highest-performing CMIP5 models in Figure 3 of Knutti et al., 2013). CESM1 consists of fully-coupled atmosphere, ocean and sea ice components with a nominal horizontal resolution of 1°. To nudge the model to winds from reanalysis, we follow the method of Blanchard-Wrigglesworth et al. (2021) and Roach and Blanchard-Wrigglesworth (2022), which is similar to that used by Jung et al. (2014), Ding et al. (2017), and references therein. We contrast results with the CESM1 LENS (Kay et al., 2015), a set of 35 simulations with identical physics and driven by identical radiative forcing that differ only at round-off level in their atmospheric initial conditions in 1920. In the ensemble mean of these 35 experiments (denoted LENSmean), the influence of internal variability has been greatly reduced and the trend mostly reflects the true model response to climate forcing (Frankcombe et al., 2018; Swart et al., 2015). Wind nudging simulations use initial conditions from LENS.

Letting $x(t)$ denote the model state vector at model timestep t and $F(x)$ the internal tendency of the system, nudging occurs via

$$\frac{dx}{dt} = F(x) + F_{\text{nudge}}.$$

The nudging term F_{nudge} is proportional to the difference between the target analysis at a future analysis timestep, $O\left(t'_{\text{next}}\right)$, and the model state at the current timestep, $x(t)$,

$$F_{\text{nudge}} = \frac{\alpha}{\tau}\left(O\left(t'_{\text{next}}\right) - x(t)\right).$$

The nudging coefficient α is 1 everywhere within the nudging domain and changes to zero smoothly across the domain border across a buffer zone of approximately 6° (see Figure 1a in Blanchard-Wrigglesworth et al., 2021). The relaxation timescale of the nudging is $\tau = t'_{\text{next}} - t$. The atmospheric model time step is 30 min and the target analysis time step is 6 hr.

Model zonal (U) and meridional (V) winds are nudged to values from two different 6-hourly reanalyses: ERA5 (Hersbach et al., 2020), which is available from 1950 onwards and ERA-Interim (Dee et al., 2011), which is available from 1979 onwards. We denote these two sets of simulations NUDGE-ERA5 and NUDGE-ERAI

Table 1
Summary of Model Simulations

Experiment (nudging domain)	Target	No. Members (initialization)
NUDGE-ERA5 (45°–90°N and 45°–90°S)	ERA5 (1950–2018)	1 (LENS # 10)
aNUDGE-ERAI[a] (45°–90°N and 45°–90°S)	ERA-Interim anomaly	3 (LENS # 4, 21, 26)
NUDGE-ERAI[a] (45°–90°N and 45°–90°S)	ERA-Interim	3 (LENS # 6, 17, 26)
NUDGE-ERAI[a] (45°–90°N)	ERA-Interim	4 (LENS # 4, 6, 17, 26)
NUDGE-ERAI[a] (45°–60°N)	ERA-Interim	1 (LENS # 6)
NUDGE-ERAI-SH (45°–90°S)	ERA-Interim	3 (LENS # 6, 17, 26)
aNUDGE-ERAI-60 (60°–90°N) and 60°–90°S	ERA-Interim anomaly	3 (LENS # 6, 17, 21)

Note. All experiments span 1979–2018 unless noted.
[a]= included in NUDGE-ERAI ensemble mean.

respectively. Wind nudging is imposed over various spatial domains as listed in Table 1 at all vertical levels above 850 hPa, throughout the time period for which each reanalysis is available (1950–2018 for NUDGE-ERA5 and 1979–2018 for NUDGE-ERAI). The configuration and radiative forcings are otherwise identical to LENS, that is, with historical forcing before 2005 and RCP8.5 from 2006 to 2018. We mostly focus on simulations where winds are nudged polewards of 45°, but include results from simulations where nudging is applied over other spatial domains (see Table 1). We found that nudging equatorward of 45° resulted in unphysical model drifts.

We find that the simulation of AMOC is similar whether winds are nudged toward absolute values from reanalysis or toward departures from the reanalysis climatology (i.e., the target constructed as the sum of model climatology over 1979–2018 and reanalysis anomalies) (Figure S1 in Supporting Information S1). Therefore, we do not distinguish between these sets of experiments in Section 3. Ensemble members with wind nudging initialized from different LENS members show close agreement (Figure S1 in Supporting Information S1), demonstrating that the impact of internal variability arising from differences in initial conditions is small in this experimental configuration. To determine the length of adjustment to the onset of wind nudging, we compare the AMOC timeseries of the simulation with wind nudging beginning in 1950 to those beginning in 1979. These converge from year 2004 onwards, so the first 25 years of each nudging simulation are discarded to allow for spin-up.

We compare wind nudging simulations to monthly mean observations from the RAPID array (Frajka-Williams et al., 2021, with calculation described in McCarthy et al., 2015), which provides estimates of the AMOC at 26.5°N from May 2004 to present, with an annual estimate of observational uncertainty from McCarthy et al. (2015). Sinha et al. (2018) suggest that the interannual variability captured by RAPID is accurate. We also include output from the CESM1 forced-ocean simulation (Large and Yeager, 2009, as described in Kim et al., 2018). In this simulation, the CESM1 ocean component is forced by the Coordinated Ocean-Ice Reference Experiments (CORE) interannually-varying atmospheric data set, which has now been extended to cover 1958–2016. This forced-ocean simulation is denoted FO-CORE. The common period of simulations and observations used for most analysis is thus May 2004–December 2016 (see Figure S2 in Supporting Information S1 for the full RAPID timeseries). For consistency with observations, we compute the AMOC at 26.5°N from all model output using the RAPID method with the package provided by Roberts et al. (2013), which includes a calculation of the Ekman component of AMOC arising from wind stress (described in SI of Roberts et al., 2013).

3. Results

3.1. AMOC in RAPID and LENS

We begin by comparing AMOC at 26.5°N in the fully-coupled CESM1 LENS and in the RAPID array. Figure 1a shows timeseries of monthly AMOC smoothed with a 12-month rolling mean over May 2004–December 2016, the period where data are available from RAPID and from all the CESM1 simulations. Over this period, the RAPID observations exhibit pronounced interannual variability (Figure 1c, black circle), whereas the 35 individual LENS members show lower interannual variability (Figure 1c, blue lines). As expected—since LENS is a free-running ensemble—interannual variability in LENS is uncorrelated with RAPID (Figure 1b, blue lines).

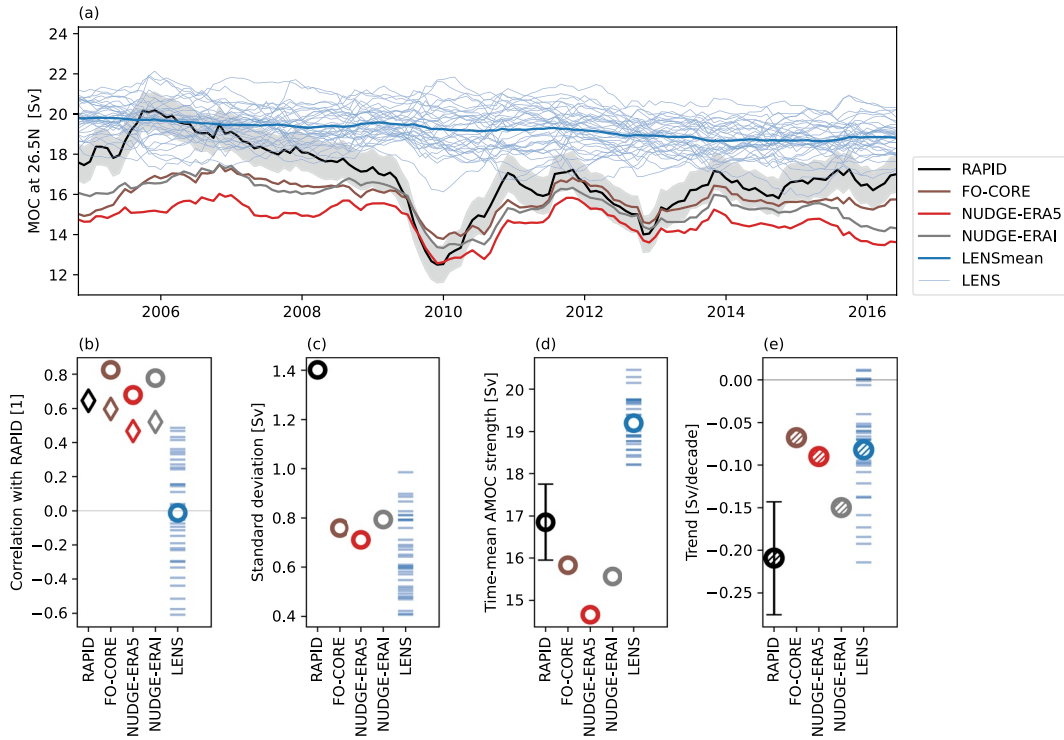

Figure 1. Comparison of model experiments with RAPID observations for monthly means over May 2004–December 2016 with a 12-month rolling mean. (a) Atlantic Meridional Overturning Circulation timeseries. (b) Correlation of detrended timeseries with RAPID. Diamonds mark the correlation between the RAPID AMOC and the Ekman component of RAPID, FO-CORE, NUDGE-ERA5, and NUDGE-ERAI respectively. (c) Standard deviation of detrended timeseries. (d) Time-mean value of timeseries. (e) Linear trend, with hatching on circles marking trends that are statistically significant at the 95% level. The error bar of 0.9 Sv on RAPID data in (d) is from (McCarthy et al., 2015). The error bar on RAPID trends in (e) is the range of all trends computed from 1,000 synthetic timeseries (RAPID data plus random noise with a standard deviation of 0.9 Sv). NUDGE-ERAI represents the mean of all simulations that include nudging between 45° and 60°N (Table 1). NUDGE-ERA5 and FO-CORE represent one simulation each.

All members of LENS show a high time-mean magnitude of AMOC at 26.5°N (Figure 1d, blue lines). Over the RAPID period, the LENS ensemble-mean time-mean strength is 19.2 Sv, and the time-means of all individual members are larger than the observed time-mean strength of 16.9 ± 0.9 Sv (Figure 1d). Considering the vertical profile of the mean overturning strength (Figure S3 in Supporting Information S1), LENS has stronger northward transport than RAPID in the upper ocean, and stronger southward transport at depth. Over 2004–2016, the trend in AMOC in the LENS ensemble-mean is weakly negative, with less than half the magnitude of the decline shown in RAPID (Figure 1e). Only five LENS ensemble members have trends within the uncertainty range of RAPID. In summary, LENS has lower, randomly-phased interannual variability, a stronger mean amplitude, and most ensemble members have a weaker decline in the AMOC at 26.5°N than the RAPID observations. Next, we consider how the variability, mean strength and trends in AMOC are impacted by the application of wind-nudging in the CESM1 fully-coupled model (NUDGE-ERA5 and NUDGE-ERAI), and how these results compare with the CESM1 FO-CORE.

3.2. AMOC in NUDGE and FO

3.2.1. Interannual Variability

Nudging the circulation in a specific domain in atmospheric models affects the circulation outside the domain, via the transport of information across the domain boundaries (e.g., Jung et al., 2010; Liu et al., 2021). We find that wind-nudging in the mid-latitudes has strong non-local impacts on atmospheric circulation at subtropical latitudes (Figures S4–S5 in Supporting Information S1). Teleconnections are especially pronounced when the nudging domain spans regions where Rossby waves are initiated, such as the midlatitude jet. The correlation of surface

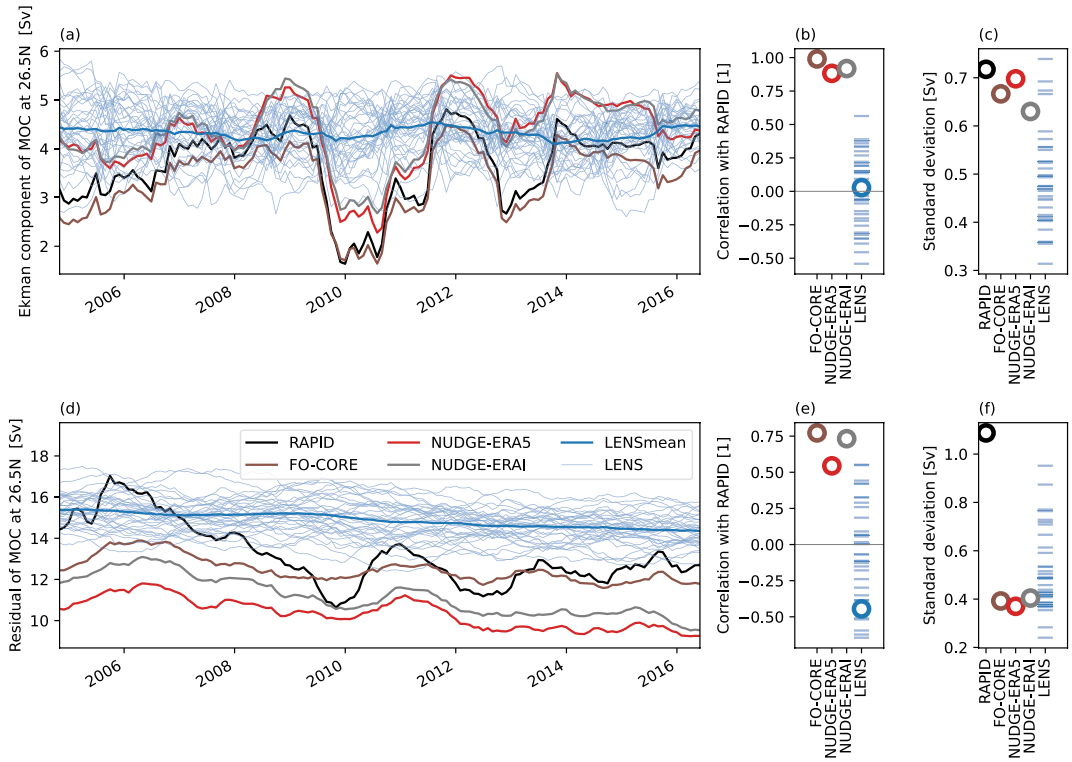

Figure 2. Comparison of model experiments with RAPID observations over May 2004–December 2016. (Top panel) Ekman component of AMOC at 26.5°N, with a 12-month rolling mean (Bottom panel) the residual component of AMOC at 26.5°N (Figure 1a minus panel (a) in this figure). (a and d) Timeseries, (b and e) correlation with corresponding timeseries from RAPID, both detrended, and (c and f) standard deviation of detrended timeseries.

zonal winds with ERA-Interim reanalysis in the Atlantic basin at 26°N—outside the nudging domain—exceeds 0.7 in all simulations that nudge over 45°–60°N (Figure S4 in Supporting Information S1). AMOC variability in simulations with wind nudging applied north of 60°N or only in the Southern Hemisphere is indistinguishable from LENS (Figure S2 in Supporting Information S1), suggesting that the influence of winds over 45°–60°N is key. Indeed, applying wind nudging only between 45° and 60°N results in a similar simulation of AMOC at 26.5°N as when nudging is applied polewards of 45° (Figures S2 and S4–S6 in Supporting Information S1). We therefore group together all simulations that include nudging over 45°–60°N in the following analysis.

FO-CORE captures the majority of the observed phasing of AMOC (correlation $R = 0.82$, Figure 1b). The coupled wind-nudging simulations that nudge north of 45°N (NUDGE-ERAI and NUDGE-ERA5) also capture much of the observed phasing of AMOC, including the low of 2010. The correlation with RAPID is $R = 0.78$ for NUDGE-ERAI and $R = 0.68$ for NUDGE-ERA5 (Figure 1b). This agreement with observations highlights the importance of observed atmospheric circulation variability for AMOC variations. Previous studies have found similar results using forced-ocean simulations with and without ocean data assimilation (e.g., Roberts et al., 2013), and here we demonstrate this result using a coupled model and show that this is largely a result of the wind-driven circulation (which can modify both momentum and buoyancy forcing).

Previous studies have found that Ekman transports driven directly by the wind play a dominant role in intra-annual AMOC variability (e.g., Cabanes et al., 2008). Figure 2 shows the Ekman component of AMOC at 26.5°N and the residual (total AMOC minus Ekman component). The low of 2010 concurrent with the record low NAO (Osborn, 2011) is particularly noticeable, and is well-captured by both the wind-nudging simulations and FO-CORE. The correlation between the full AMOC from RAPID (black line, Figure 1a) and the Ekman component of the simulated AMOC (Figure 2a) is 0.60 for FO-CORE, 0.47 for NUDGE-ERA5 and 0.52 for NUDGE-ERAI (diamonds in Figure 1b). Therefore a large portion of the agreement of modeled AMOC variability with observations arises from the instantaneous impact of wind forcing on Ekman transport locally (i.e., at 26.5°N).

Although the phasing of interannual variability is well-captured, the level of variability in the smoothed monthly timeseries from FO-CORE, NUDGE-ERAI, and NUDGE-ERA5 is similar to LENS, which is biased low relative to RAPID (Figure 1c). This bias appears only in the non-Ekman component (Figure 2). Moreover, longer-term multi-decadal variability remains lower than that from the RAPID array in all model simulations (Figure S2 in Supporting Information S1 and Figure 2d). Our results suggest that these apparent biases are not solely attributable to biases in the mid-to-high latitude atmospheric circulation, as simulated biases in AMOC interannual variance and multi-decadal variability persist when wind-nudging is applied. Simulating realistic variance in the NAO does not improve the underestimation of low-frequency variability in AMOC in CESM1, in contrast to the suggestion of Kim et al. (2018). The reduced AMOC variability in models compared to RAPID is particularly apparent in 2006, when the observed record-high AMOC strength is not captured by either the forced-ocean or wind-nudging simulations. This mismatch may arise from low spatial resolution in the model, processes unrelated to winds or climate forcing (e.g., aerosol changes, Menary et al., 2020) not captured by CESM1.

3.2.2. Mean Strength

Wind-nudging improves the phasing of interannual AMOC variability. How does it impact the time-mean strength? Figure 1a shows a striking reduction in AMOC magnitude in the wind-nudging (north of 45°N) and forced-ocean simulations as compared with LENS. The wind-nudging and forced-ocean simulations fall below the observational range, with magnitudes of 14.7 Sv, 15.6 Sv, and 15.8 Sv for NUDGE-ERA5, NUDGE-ERAI and FO-CORE respectively, as compared with 16.9 ± 0.9 Sv for RAPID (Figure 1d), suggesting that wind biases may be responsible for a large portion of time-mean AMOC biases in coupled models. Although biased low, these simulations are in marginally better agreement with RAPID than the LENSmean, which has a magnitude of 19.2 Sv. A large part of the discrepancy occurs during the observed high in 2006 (Figure 1a). In the time-mean overturning strength as a function of depth (Figure S3 in Supporting Information S1), the wind-nudging simulations are in closer agreement with RAPID in the upper 2000 m than LENS, but do not improve at depths below 2,000 m.

Previous studies have found that decadal AMOC variability primarily arises from water mass transformation driven by surface buoyancy fluxes in the subpolar gyre (Delworth et al., 2016; Oldenburg et al., 2021, 2022; Yeager & Danabasoglu, 2014). To test whether this mechanism may also impact the 2004–2016 mean, we compute a mean surface buoyancy flux B over the subpolar gyre (defined as 50°–65°N, 295°–340°E), combining the influence of heat and freshwater into a single "heat-equivalent" quantity. We find that the mean B simulated by the wind-nudging (north of 45°N) and forced-ocean simulations is substantially reduced compared to LENS ensemble members (Figure 3a). Our results confirm the importance of westerly winds and their associated influence on buoyancy over the subpolar gyre for the AMOC at 26.5°N. Furthermore, Figure 3 highlights the relationship between mean buoyancy fluxes and mean AMOC for 2004–2016, while previous studies have focused on the relationship between variability in these quantities.

When decomposing the heat and freshwater effects on B separately in Figures 3b and 3c, following Cerovečki et al. (2011) (Text S1 in Supporting Information S1), we see that the heat component is key to the differences in B, with only small differences in the freshwater component. This is consistent with large declines in surface turbulent heat fluxes over the subpolar gyre relative to LENS (lower-left panels in Figure S7 in Supporting Information S1). The surface turbulent heat fluxes depend on the coupled temperature and humidity response at the surface, as well as the wind changes. Although the winds remain mostly within the range of LENS, the surface turbulent heat fluxes decrease below the range of LENS due to the coupled temperature and humidity response to the changes in winds. These impacts are similar whether nudging to the full reanalysis winds or their anomalies, as the climatology correction applied in the latter case is small relative to the wind variability (top-left panels in Figure S7 in Supporting Information S1).

3.2.3. Trends

Wind-nudging improves the simulation of AMOC variability and significantly reduces the magnitude of AMOC by reducing surface buoyancy fluxes in the subpolar gyre. Does it influence trends in AMOC? Over 2004–2016, LENS generally shows weaker trends than RAPID, but with several ensemble members falling within the range of observational uncertainty in the trends (Figure 1e). The trend in FO-CORE is close to the LENS mean. NUDGE-ERA5 has a very slightly stronger decline than FO-CORE, and NUDGE-ERAI has a stronger decline than both, falling within the uncertainty range of RAPID. Thus there is a modest improvement in AMOC trends

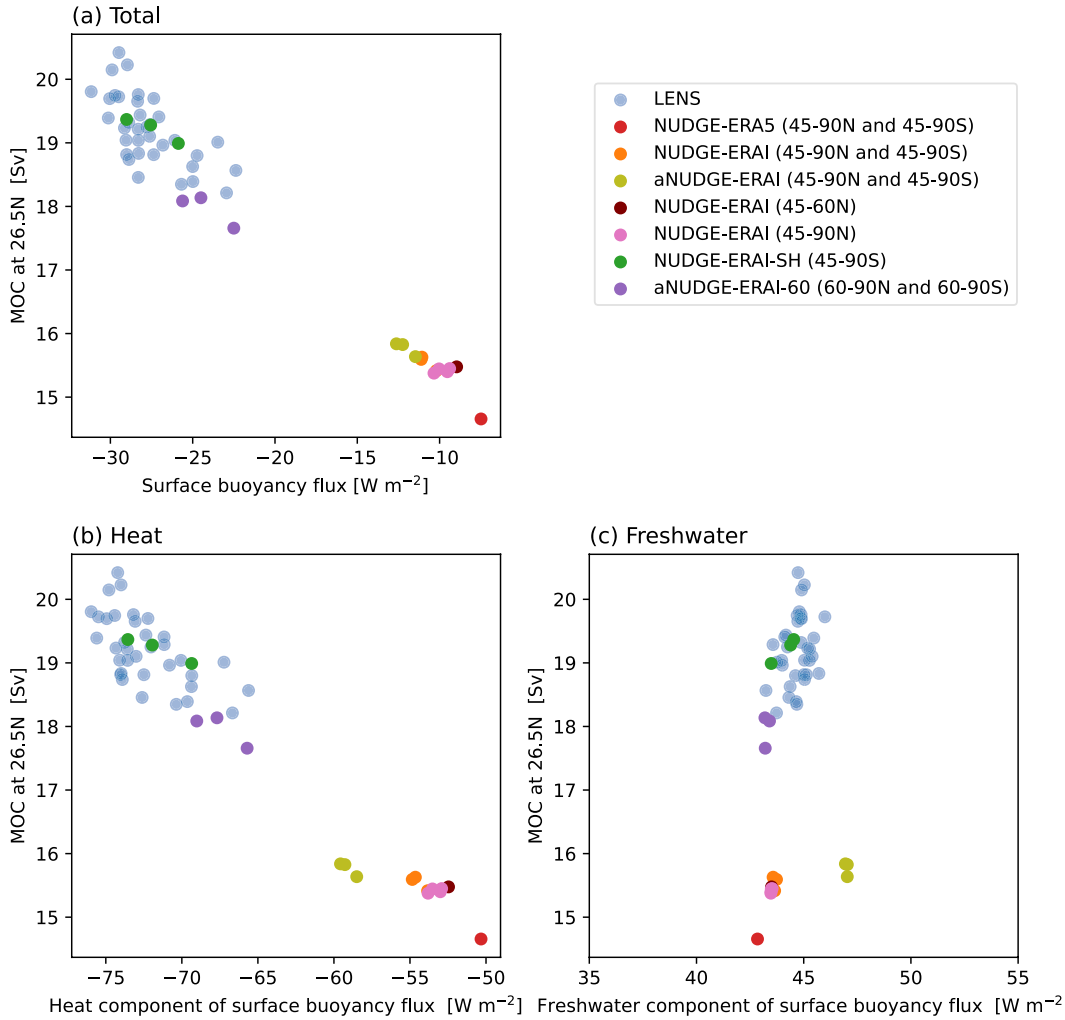

Figure 3. Atlantic Meridional Overturning Circulation at 26.5°N versus the surface buoyancy flux over the subpolar gyre for the 2004–2016 mean, for (a) the total, (b) the heat component, and (c) the freshwater component. Note the differing scales of the *x*-axes.

when nudging toward observed circulation, but by an amount that is sensitive to the choice of reanalysis product. Trends in the Ekman component of AMOC over 2004–2016 in FO-CORE, NUDGE-ERAI, and NUDGE-ERA5 are positive and similar to RAPID, while the Ekman component of AMOC for the LENS mean has zero trend (Figure S8b in Supporting Information S1). The trends in AMOC are dominated by the trends in the residual (non-Ekman) component, and these are more negative in FO-CORE, NUDGE-ERAI, and NUDGE-ERA5 than LENSmean, yet still not as negative as RAPID (Figure S8c in Supporting Information S1).

Over the longer period of 1979–2016, LENS has a trend of −0.05 Sv/decade, NUDGE-ERA5 has a statistically insignificant negative trend and FO-CORE has a small positive trend of 0.02 Sv/decade (Figure S8d in Supporting Information S1) (Note that the NUDGE-ERAI simulations are only analyzed from 2004 onwards.) Therefore, constraining winds in a model toward observations dampens the AMOC decline simulated by LENS over this period. There are also impacts of constraining the winds on North Atlantic sea surface temperatures (Figure S9 in Supporting Information S1). The LENSmean features an area of cooling in the North Atlantic that is not observed in the HADISST data set, likely related to the negative trends in AMOC in LENS over 1979–2016. NUDGE-ERA5 still has an area of cooling but it is smaller in area, although stronger in magnitude and shifted southwards, near the boundary of the nudging domain. NUDGE-ERA5 has areas of warming south of Greenland that appear closer to HADISST than the LENSmean and FO-CORE in some regions, but overestimates the warming signal in others.

4. Conclusions

In this study, we examine AMOC at 26.5°N in three types of experiments with CESM1: the fully-coupled large ensemble (LENS), the forced-ocean configuration (FO-CORE) where the whole atmosphere is specified by the CORE reanalysis, and new experiments where meridional and zonal winds above the boundary layer and polewards of 45° are nudged to values from the ERA5 (NUDGE-ERA5) or ERA-Interim (NUDGE-ERAI) reanalyses. In the wind-nudging simulations, the influence of constraining the winds extends beyond the nudging domain due to advection of heat, moisture, and momentum across the perimeter of the nudging domain. Even nudging only between 45 and 60°N results in an AMOC that falls outside the range of the CESM1 LENS, indicating that the subpolar jet region is particularly important. The AMOC in simulations where nudging is applied polewards of 60° or in the Southern Hemisphere only are not statistically distinguishable from LENS in either variability or magnitude.

We find that correcting biases in simulated winds polewards of 45°N substantially improves biases in AMOC at 26.5°N in CESM1 compared to observations from the RAPID array. Specifically, the phasing of interannual variability is well-captured and the time-mean AMOC magnitude is closer to observations. The trend over the observational period in NUDGE-ERAI is within the range of observational uncertainty, as are 5 of the 35 LENS members, but not NUDGE-ERA5 or FO-CORE. Besides the difference in trends, we come to similar conclusions about how winds control AMOC when nudging to either ERA-Interim or ERA5, strengthening the robustness of our findings. That we obtain broadly similar results with the wind-nudging and forced-ocean simulations suggests that the large-scale atmospheric circulation variability is a powerful driver of AMOC, and that prescribing the complete atmospheric surface conditions down to the ocean-atmosphere interface (as in FO-CORE) has limited additional impact on AMOC over the RAPID era. It is well-established that buoyancy fluxes over the subpolar gyre are a driver of AMOC variability. Here we show that changes in turbulent heat fluxes associated with the observed winds drive a reduction of around 20% in the time-mean AMOC strength relative to the LENS ensemble-mean.

Overall, the AMOC at 26.5°N in wind-nudging simulations is in closer agreement with AMOC metrics in the RAPID array than several ocean reanalyses (Karspeck et al., 2017). Despite these successes, however, longer-timescale variability in the non-Ekman component is underestimated by both the forced-ocean and wind-nudging experiments, showing that model biases in the low frequency variability are largely not due to biases in atmospheric circulation north of 45°N. Our inability to simulate the large change in AMOC over 2006–2010 despite nudging to the observed winds should motivate further research into the causes of this important model bias.

Over 1979 to present, direct observations of AMOC are not available, and there is no evidence to suggest that AMOC has declined over this period (Jackson et al. (2022) and references therein). The LENS mean simulates a negative forced trend in the AMOC at 26.5°N over 1979–2016 and a cooling trend in the North Atlantic that is not seen in observations. Nudging winds polewards of 45°N yields a statistically insignificant trend in AMOC and sea surface temperature trends in the North Atlantic that are in some aspects in better agreement with observations. Our results suggest that the CESM1 LENS may be biased toward an AMOC decline over the satellite era that has not occurred in the real world partially as a result of model biases in the atmosphere, with winds playing a significant role. This suggests that improvement in the representation of the high-latitude atmosphere is important for future climate projections.

Data Availability Statement

All data in this study is publicly available. ERA-Interim (European Centre for Medium-range Weather Forecast (ECMWF, 2011) and ERA5 (Bell et al., 2021) are from ECMWF. The CESM1 LENS (Kay et al., 2015) is publicly available via https://www.cesm.ucar.edu/projects/community-projects/LENS/data-sets.html. Data from the RAPID array is provided by Frajka-Williams et al. (2021). We use sea surface temperatures from HadISST 1.1 (Rayner, 2003) from http://www.metoffice.gov.uk/hadobs/hadisst [accessed Feb 2021]. Model output is available at https://doi.org/10.5281/zenodo.7343036.

Acknowledgments
The authors would like to acknowledge computing and data storage resources, including the Cheyenne supercomputer (https://doi.org/10.5065/D6RX99HX) provided by the Computational and Information Systems Laboratory at National Center for Atmospheric Research (NCAR). The Community Earth System Model (CESM) project is supported primarily by the National Science Foundation (NSF); this material is based upon work supported by the NCAR, which is a major facility sponsored by the NSF under Cooperative Agreement 1852977. We thank the Polar Climate Working Group at NCAR. We also thank Ian Eisenman, Mitchell Bushuk, and Elizabeth Maroon for helpful discussions. LR, EBW, WC, and CMB were supported by National Oceanic and Atmospheric Administration (NOAA) MAPP Grant NA18OAR4310274. LR was also supported by 80NSSC20M0282 and the NOAA Climate and Global Change Postdoctoral Fellowship Program, which is administered by UCAR's Cooperative Programs for the Advancement of Earth System Science under award NA18NWS4620043B. EBW was also supported by NSF award OPP-2213988. SR and KCA acknowledge support from NSF Award OCE-1850900. This publication is PMEL Contribution 5442, and is partially funded by the Cooperative Institute for Climate, Ocean, Ecosystem Studies under NOAA Cooperative Agreement NA20OAR4320271, Contribution No. 2022–1228. Research was supported by the NASA Modeling Analysis and Prediction program.

References

Bell, B., Hersbach, H., Berrisford, P., Dahlgren, P., Horányi, A., Muñoz Sabater, J., et al. (2021). ERA5 Complete Preliminary: Fifth generation of ECMWF atmospheric reanalyses of the global climate from 1950 to 1978 (preliminary version). [accessed Mar 2022] [Dataset]. Change. Retrieved from https://www.ecmwf.int/en/forecasts/datasets/reanalysis-datasets/era5

Blanchard-Wrigglesworth, E., Roach, L. A., Donohoe, A., & Ding, Q. (2021). Impact of winds and Southern Ocean SSTs on Antarctic sea ice trends and variability. *Journal of Climate*, *34*(3), 1–47. https://doi.org/10.1175/JCLI-D-20-0386.1

Buckley, M. W., & Marshall, J. (2016). Observations, inferences, and mechanisms of the Atlantic Meridional Overturning Circulation: A review. *Reviews of Geophysics*, *54*(1), 5–63. https://doi.org/10.1002/2015RG000493

Cabanes, C., Lee, T., & Fu, L.-L. (2008). Mechanisms of interannual variations of the Meridional Overturning Circulation of the North Atlantic Ocean. *Journal of Physical Oceanography*, *38*(2), 467–480. https://doi.org/10.1175/2007JPO3726.1

Cerovečki, I., Talley, L. D., & Mazloff, M. R. (2011). A comparison of Southern Ocean air-sea buoyancy flux from an ocean state estimate with five other products. *Journal of Climate*, *24*(24), 6283–6306. https://doi.org/10.1175/2011JCLI3858.1

Cheng, W., Chiang, J. C. H., & Zhang, D. (2013). Atlantic meridional overturning circulation (AMOC) in CMIP5 models: RCP and historical simulations. *Journal of Climate*, *26*(18), 7187–7197. https://doi.org/10.1175/JCLI-D-12-00496.1

Dee, D. P., Uppala, S. M., Simmons, A. J., Berrisford, P., Poli, P., Kobayashi, S., et al. (2011). The ERA-interim reanalysis: Configuration and performance of the data assimilation system. *Quarterly Journal of the Royal Meteorological Society*, *137*(656), 553–597. https://doi.org/10.1002/qj.828

Delworth, T. L., Zeng, F., Vecchi, G. A., Yang, X., Zhang, L., & Zhang, R. (2016). The North Atlantic Oscillation as a driver of rapid climate change in the northern Hemisphere. *Nature Geoscience*, *9*(7), 509–512. https://doi.org/10.1038/ngeo2738

Ding, Q., Schweiger, A., L'Heureux, M., Battisti, D. S., Po-Chedley, S., Johnson, N. C., et al. (2017). Influence of high-latitude atmospheric circulation changes on summertime Arctic sea ice. *Nature Climate Change*, *7*(4), 289–295. https://doi.org/10.1038/nclimate3241

European Centre for Medium-range Weather Forecast (ECMWF). (2011). The ERA-Interim reanalysis dataset [accessed Jan 2020] [Dataset]. Change. Retrieved from https://www.ecmwf.int/en/forecasts/datasets/archive-datasets/reanalysis-datasets/era-interim

Fox-Kemper, B., Hewitt, H. T., Xiao, C., Aðalgeirsdóttir, G., Drijfhout, S. S., Edwards, T. L., et al. (2021). Ocean, cryosphere and sea level change. In I. P. o. C. Change (Ed.), *Climate change 2021: The physical science basis*. Cambridge University Press.

Frajka-Williams, E., Moat, B. I., Smeed, D. A., Rayner, D., Johns, W. E., Baringer, M. O., et al. (2021). *Atlantic Meridional Overturning Circulation observed by the RAPID-MOCHA-WBTS (RAPID-Meridional overturning circulation and heatflux array-western boundary time series) array at 26N from 2004 to 2020* (v2020.1) [accessed Jul 2022] [Dataset]. British Oceanographic Data Centre - Natural Environment Research Council. https://doi.org/10.5285/cc1e34b3-3385-662b-e053-6c86abc03444

Frankcombe, L. M., England, M. H., Kajtar, J. B., Mann, M. E., Steinman, B. A., Frankcombe, L. M., & Steinman, B. A. (2018). On the choice of ensemble mean for estimating the forced signal in the presence of internal variability. *Journal of Climate*, *31*(14), 5681–5693. https://doi.org/10.1175/JCLI-D-17-0662.1

Hersbach, H., Bell, B., Berrisford, P., Hirahara, S., Horányi, A., Muñoz-Sabater, J., et al. (2020). The ERA5 global reanalysis. *Quarterly Journal of the Royal Meteorological Society*, *146*(730), 1999–2049. https://doi.org/10.1002/qj.3803

Hurrell, J. W., Holland, M. M., Gent, P. R., Ghan, S., Kay, J. E., Kushner, P. J., et al. (2013). The community Earth system model: A framework for collaborative research. *Bulletin of the American Meteorological Society*, *94*(9), 1339–1360. https://doi.org/10.1175/BAMS-D-12-00121.1

Jackson, L. C., Biastoch, A., Buckley, M. W., Desbruyčres, D. G., Frajka-Williams, E., Moat, B., & Robson, J. (2022). The evolution of the North Atlantic meridional overturning circulation since 1980. *Nature Reviews Earth & Environment*, *3*(4), 241–254. https://doi.org/10.1038/s43017-022-00263-2

Jung, T., Kasper, M. A., Semmler, T., & Serrar, S. (2014). Arctic influence on subseasonal midlatitude prediction. *Geophysical Research Letters*, *41*(10), 3676–3680. https://doi.org/10.1002/2014GL059961

Jung, T., Miller, M. J., & Palmer, T. N. (2010). Diagnosing the origin of extended-range forecast errors. *Monthly Weather Review*, *138*(6), 2434–2446. https://doi.org/10.1175/2010MWR3255.1

Karspeck, A. R., Stammer, D., Köhl, A., Danabasoglu, G., Balmaseda, M., Smith, D. M., et al. (2017). Comparison of the Atlantic meridional overturning circulation between 1960 and 2007 in six ocean reanalysis products. *Climate Dynamics*, *49*(3), 957–982. https://doi.org/10.1007/s00382-015-2787-7

Kay, J. E., Deser, C., Phillips, A., Mai, A., Hannay, C., Strand, G., et al. (2015). The community Earth system model (CESM) large ensemble project: A community resource for studying climate change in the presence of internal climate variability. *Bulletin of the American Meteorological Society*, *96*(8), 1333–1349. https://doi.org/10.1175/BAMS-D-13-00255.1

Kim, W. M., Yeager, S., Chang, P., & Danabasoglu, G. (2018). Low-frequency North Atlantic climate variability in the community Earth system model large ensemble. *Journal of Climate*, *31*(2), 787–813. https://doi.org/10.1175/JCLI-D-17-0193.1

Knutti, R., Masson, D., & Gettelman, A. (2013). Climate model genealogy: Generation CMIP5 and how we got there. *Geophysical Research Letters*, *40*(6), 1194–1199. https://doi.org/10.1002/grl.50256

Kostov, Y., Johnson, H. L., Marshall, D. P., Heimbach, P., Forget, G., Holliday, N. P., et al. (2021). Distinct sources of interannual subtropical and subpolar Atlantic overturning variability. *Nature Geoscience*, *5*(7), 491–495. https://doi.org/10.1038/s41561-021-00759-4

Large, W. G., & Yeager, S. G. (2009). The global climatology of an interannually varying air–sea flux data set. *Climate Dynamics*, *33*(2–3), 341–364. https://doi.org/10.1007/s00382-008-0441-3

Larson, S. M., Buckley, M. W., & Clement, A. C. (2020). Extracting the buoyancy-driven Atlantic Meridional Overturning circulation. *Journal of Climate*, *33*(11), 4697–4714. https://doi.org/10.1175/JCLI-D-19-0590.1

Liu, Z., Bollasina, M. A., Wilcox, L. J., Rodríguez, J. M., & Regayre, L. A. (2021). Contrasting the role of regional and remote circulation in driving Asian Monsoon biases in MetUM GA7.1. *Journal of Geophysical Research: Atmospheres*, *126*(14), e2020JD034342. https://doi.org/10.1029/2020JD034342

McCarthy, G. D., Smeed, D. A., Johns, W. E., Frajka-Williams, E., Moat, B. I., Rayner, D., et al. (2015). Measuring the Atlantic Meridional Overturning circulation at 26°N. *Progress in Oceanography*, *130*, 91–111. https://doi.org/10.1016/j.pocean.2014.10.006

Menary, M. B., Robson, J., Allan, R. P., Booth, B. B. B., Cassou, C., Gastineau, G., et al. (2020). Aerosol-forced AMOC changes in CMIP6 historical simulations. *Geophysical Research Letters*, *47*(14), e2020GL088166. https://doi.org/10.1029/2020GL088166

Oldenburg, D., Wills, R. C. J., Armour, K. C., & Thompson, L. (2022). Resolution dependence of atmosphere–ocean interactions and water mass transformation in the North Atlantic. *Journal of Geophysical Research: Oceans*, *127*(4). https://doi.org/10.1029/2021jc018102

Oldenburg, D., Wills, R. C. J., Armour, K. C., Thompson, L., & Jackson, L. C. (2021). Mechanisms of low-frequency variability in North Atlantic Ocean heat transport and AMOC. *Journal of Climate*, *34*(12), 4733–4755. https://doi.org/10.1175/JCLI-D-20-0614.1

Osborn, T. J. (2011). Winter 2009/2010 temperatures and a record-breaking North Atlantic Oscillation index. *Weather*, *66*(1), 19–21. https://doi.org/10.1002/wea.660

Rayner, N. A. (2003). Global analyses of sea surface temperature, sea ice, and night marine air temperature since the late nineteenth century. *Journal of Geophysical Research*, *108*(D14), 4407. https://doi.org/10.1029/2002JD002670

Roach, L. A., & Blanchard-Wrigglesworth, E. (2022). Observed winds crucial for September Arctic sea ice loss. *Geophysical Research Letters*, *49*(6). https://doi.org/10.1029/2022gl097884

Roberts, C. D., Jackson, L., & McNeall, D. (2014). Is the 2004-2012 reduction of the Atlantic Meridional Overturning Circulation significant? *Geophysical Research Letters*, *41*(9), 3204–3210. https://doi.org/10.1002/2014GL059473

Roberts, C. D., Waters, J., Peterson, K. A., Palmer, M. D., McCarthy, G. D., Frajka-Williams, E., et al. (2013). Atmosphere drives recent interannual variability of the Atlantic Meridional Overturning Circulation at 26.5°N. *Geophysical Research Letters*, *40*(19), 5164–5170. https://doi.org/10.1002/grl.50930

Sinha, B., Smeed, D., McCarthy, G., Moat, B., Josey, S., Hirschi, J.-M., et al. (2018). The accuracy of estimates of the overturning circulation from basin-wide mooring arrays. *Progress in Oceanography*, *160*, 101–123. https://doi.org/10.1016/j.pocean.2017.12.001

Swart, N. C., Fyfe, J. C., Hawkins, E., Kay, J. E., & Jahn, A. (2015). Influence of internal variability on Arctic sea-ice trends. *Nature Climate Change*, *5*(2), 86–89. https://doi.org/10.1038/nclimate2483

Wang, X., Li, J., Sun, C., & Liu, T. (2017). NAO and its relationship with the Northern Hemisphere mean surface temperature in CMIP5 simulations. *Journal of Geophysical Research*, *122*(8), 4202–4227. https://doi.org/10.1002/2016JD025979

Weijer, W., Cheng, W., Garuba, O. A., Hu, A., & Nadiga, B. T. (2020). CMIP6 models predict significant 21st century decline of the Atlantic meridional overturning circulation. *Geophysical Research Letters*, *47*(12). https://doi.org/10.1029/2019GL086075

Yan, X., Zhang, R., & Knutson, T. R. (2018). Underestimated AMOC variability and implications for AMV and predictability in CMIP models. *Geophysical Research Letters*, *45*(9), 4319–4328. https://doi.org/10.1029/2018GL077378

Yeager, S., & Danabasoglu, G. (2014). The origins of late-twentieth-century variations in the large-scale North Atlantic circulation. *Journal of Climate*, *27*(9), 3222–3247. https://doi.org/10.1175/JCLI-D-13-00125.1

Zhang, R., Sutton, R., Danabasoglu, G., Kwon, Y. O., Marsh, R., Yeager, S. G., et al. (2019). A review of the role of the Atlantic meridional overturning circulation in Atlantic multidecadal variability and associated climate impacts. *Reviews of Geophysics*, *57*(2), 316–375. https://doi.org/10.1029/2019RG000644